Polym. Bull. (2009) 62:255–270
DOI 10.1007/s00289-008-0010-2

ORIGINAL PAPER

Interfacially compatibilized LDPE/POE blends reinforced with nanoclay: investigation of morphology, rheology and dynamic mechanical properties

B. Baghaei · S. H. Jafari · H. A. Khonakdar · I. Rezaeian · L. As'habi · S. Ahmadian

Received: 21 August 2008 / Revised: 27 September 2008 / Accepted: 8 November 2008 /

Abstract Morphological, melt rheological and dynamic mechanical properties of low-density polyethylene (LDPE)/ethylene–octene copolymer (POE)/organo-montmorillonite (OMMT) nanocomposites, prepared via melt compounding were studied. The XRD traces indicated different levels of intercalated structures for the nanocomposites. Addition of a compatibilizer (PE-g-MA) improved the intercalation process. TEM results revealed existence of clay layers in both phases but they were mainly localized in the elastomeric POE phase. Addition of 5 wt% OMMT to the LDPE/POE blend led to reduction in the size of the elastomer particles confirmed by AFM. The complex viscosity and storage modulus showed little effect of the presence of the clay when no compatibilizer was added. As the extent of exfoliation increased with addition of compatibilizer, the linear viscoelastic behavior of the composites gradually changed specially at low-frequency regions. The interfacially compatibilized nanocomposites with 5 wt% OMMT had the highest melt viscosity and modulus among all the studied nanocomposites and blends. Also, this particular composition showed the best improvement in dynamic storage modulus. The results indicated that clay dispersion and interfacial adhesion, and consequently different properties of LDPE/POE/clay nanocomposites, are greatly affected by addition of compatibilizer.

Keywords Nanocomposites · Blends · LDPE · Ethylene-octene copolymer (POE) · Rheology · Morphology · Compatibilization

---

B. Baghaei · S. H. Jafari (✉) · I. Rezaeian · L. As'habi
School of Chemical Engineering, University of Tehran, Tehran, Iran
e-mail: shjafari@ut.ac.ir

H. A. Khonakdar
Iran Polymer and Petrochemical Institute, Tehran, Iran

S. Ahmadian
Institute of Biochemistry and Biophysics, University of Tehran, Tehran, Iran

Introduction

In recent years new kind of polymeric materials are emerging as polymer blends reinforced with nano-scale fillers such as organically modified clays and carbon nanotubes, which are attracting immense attention because of their remarkable properties [1–5]. These new kind of high performance materials combine the advantages of polymer blends and the merits of polymer nanocomposites. The synergistic improvement in properties, such as stiffness, gas barrier and flammability of the polymer blend/clay hybrids stems from well dispersion of clay platelets in the polymer matrices [6, 7]. Such good dispersion highly depends on interfacial energies of the system which tries to reach to a minimum interfacial energy state. For immiscible polymer blends with high interfacial energies the clay platelets with their polar nature normally tend to localize in the high polar component. If the high polar component forms the major phase then the clay platelets can be well dispersed through out the matrix [8, 9]. But when it forms the minor component the clay platelets tend to form isolated intercalated/exfoliated structures mainly within the minor phase [10]. However, in case of partially miscible blends with polar components in which the components have similar molecular structures, the interfacial energy remains low enough to accommodate the clay platelets in both the phases [11–13]. But for a partially miscible blend with nonpolar components, in spite of having low interfacial energy, the clay platelets may not have a good dispersion and they mainly remain in their original nonintercalated states [7, 14]. For such type of blends it is necessary to modify the interface through a compatibilizer [7, 14]. A maleic grafted polyolefin has been widely used as compatibilizer for polypropylene-based nanocomposites [15], but somewhat less used for polyethylene-based systems [16]. It is believed that the polar character of the anhydride causes affinity for the clay materials such that the maleated polyolefin can serve as a 'compatibilizer' between the matrix and filler [15].

Ethylene–octene copolymer (POE) developed by Dow Chemical Company using metallocene catalyst is a relatively new type of impact modifier. This copolymer has a controlled level of chain branching along the polymer backbone which makes it a good choice for impact toughening of polyolefins especially the polyethylene (PE) [17]. The impact modified polyolefins reinforced with nanoclays can be used in different applications in which a combination of flexibility and stiffness especially at low temperatures is a key point. In recent years several studies have been devoted to the toughened polypropylene/elastomer blend systems reinforced with nanoclays [18–21]. It is shown that the nanoclays could effectively compensate the reduction of modulus while keeping the toughness at a good level. LDPE/POE blend system reinforced with nanoclays, due to structural similarity between LDPE and POE, is expected to have improved properties. However, the studies on this system are rare.

Therefore, the aim of this work is to investigate the effect of blend composition, clay addition, intercalation level and compatibilizer on the melt rheological and dynamic mechanical properties of the LDPE/POE/clay nanocomposites. An attempt has been made to establish a structure-properties correlation for this hybrid system.

Experimental

Materials and melt processing

Low-density PE (LDPE) Grade LD 100MED from Exxon Mobile Chemical, with MFI of 2.0 g/10 min, density of 0.923 g/cm^3 and melting point of 109 °C and ethylene–octene copolymer (POE) Grade Engage 8100 from DuPont Dow elastomer, with MFI of 1.0 g/10 min (ASTM1238, 190 °C, 2.16 kg), density of 0.870 g/cm^3 and melting point of 55 °C were used. The compatibilizer used in this study was Fusabond E MB226DE which is a maleic anhydride modified polyethylene from DuPont with MFI of 1.5 g/10 min, density of 0.93 g/cm^3 and melting point of 122 °C. Nanomer I.44 was obtained from Nanocor. It is an ion-exchanged montmorillonite (MMT) clay with a dimethyldialkylammonium halide (70% C18, 26% C16 and 4% C14).

Nanocomposites were prepared via melt compounding using a conical twin screw micro-compounder (DACA Instrument) at 210 °C and screw speed of 100 rpm. Before melt blending the materials in a predetermined composition (see Table 1) were dry blended initially and shaken well for few minutes, then fed to the compounder.

Sample characterization

The level of intercalation and exfoliation of clay by polymer were determined by a Philips X-ray diffractometer using Cu K$_\alpha$ radiation with $\lambda = 1.54$ Å (40KV,

Table 1 Detailed compounding formulation and XRD data for nanocomposites

Sample No.	LDPE (wt%)	POE (wt%)	PE-g-MA (wt%)	Org-MMT (wt%)	(2θ) (°)	(d_{001}) (Å)
1	100	0	0	0	–	–
2	0	100	0	0	–	–
3	0	0	100	0	–	–
4	0	0	0	100	3.6	24.8
5	75	25	0	0	–	–
6	74.25	24.75	0	1	2.5	34.6
7	72.75	24.25	0	3	2.8	30.6
8	71.25	23.75	0	5	3.2	27.6
9	25	75	0	0	–	–
10	23.75	71.25	0	5	3.2	27.6
11	50	50	0	0	–	–
12	47.5	47.5	0	5	3.1	28.4
13	67.5	22.5	5	5	3.0	29.5
14	71.25	23.75	5	0	–	–
15	95	0	0	5	3.2	27.5
16	0	95	0	5	3.0	29.8
17	0	0	95	5	–	–

30 mA), The scanning was performed in 2θ range from 1° to 10° at a scanning rate of $1° \min^{-1}$.

Atomic force microscopy (AFM) was performed in a taping mode on cryofractured surface of the extruded strands using a DME microscope. A DS-95-50 scanner and a Dual Scope C26 controller were used. The dispersion of the clay platelets in the blend was studied by means of TEM. Ultra thin sections of the samples (approximately 70-nm thick) were obtained by cooling the sample in liquid nitrogen, using a Reichert om U3 ultramicrotome equipped with a diamond knife. The sections supported on 400-mesh grids were stained in OsO_4 vapors to enhance the phase contrast between the LDPE and POE. A PHILIPS CM200 FEG STEM, performing with an accelerated voltage of 200 kV was used. Rheological measurement were carried out using a MCR300 (Anton Paar) rheometer in parallel plates oscillation mode with a gap of 0.5 mm. Frequency sweeps of 100-0.1 rad/s were performed under nitrogen atmosphere at temperature of 210 °C. Dynamic mechanical analysis was performed using a Triton DMTA in bending mode with a single cantilever. A frequency of 1 Hz, a temperature range of −150 to 100 °C and a heating rate of $2\ \mathrm{K}\ \min^{-1}$ were used.

Results and discussion

Structural analysis of the nanocomposites using X-ray diffraction

Figure 1 shows XRD patterns of the neat organically modified montmorillonite (OMMT) and nanocomposites of LDPE, POE, PE-g-MA with 5% OMMT. The XRD pattern of the OMMT shows an intensive peak at 2θ around 3.6°, corresponding to a basal spacing of 24.8 Å. When OMMT is added to the LDPE, this peak shifts to lower angle and appears at around 3.2° corresponding to a basal spacing of 27.5 Å. The increase in spacing is an indication of intercalation of polymer into the interlayer galleries of the clay. Similar results have been reported for other polyolefins nanocomposites prepared by using Nanomer [22, 23]. As it can be seen from Fig. 1, the POE/clay 95/5 nanocomposite shows a broad peak at a slightly lower angle than the LDPE/clay nanocomposite. This may be attributed to the regular chain branching of POE in contrast to LDPE which has random chain branching along the polymer backbone. Polymer with narrower molecular weight distribution exhibits less shear thinning during extrusion and this is the case for POE. The increase in apparent viscosity during extrusion results in higher shear stresses, which may be responsible for the improved interlayer separation of the metallocene-based nanocomposite. Additionally, the regular chain branching of the metallocene POE would lead to an increase in the chain entanglement which is apparent if one compares the melt viscosity of the neat POE with that of LDPE, this in turn will increase shear stress and hence leads to improved delamination of the clay layers in POE/clay system [24].

The PE-g-MA/clay 95/5 nanocomposite shows almost complete exfoliation structure. Absence of the basal peak in PE-g-MA/clay system is an indication of enhanced interaction between the PE-g-MA and clay.

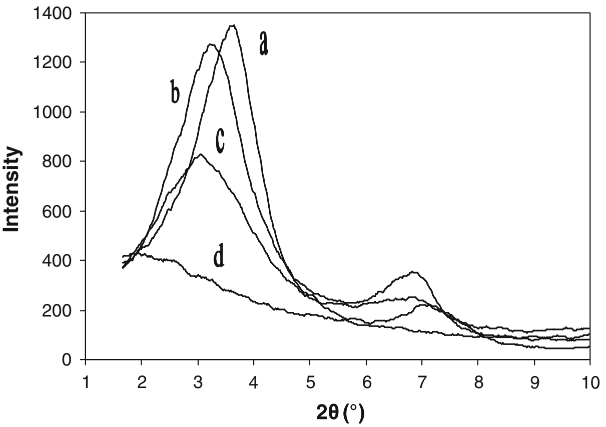

Fig. 1 XRD patterns of **a** organoclay, **b** LDPE/clay 95/5, **c** POE/clay 95/5, **d** PE-g-MA/clay 95/5 nanocomposites

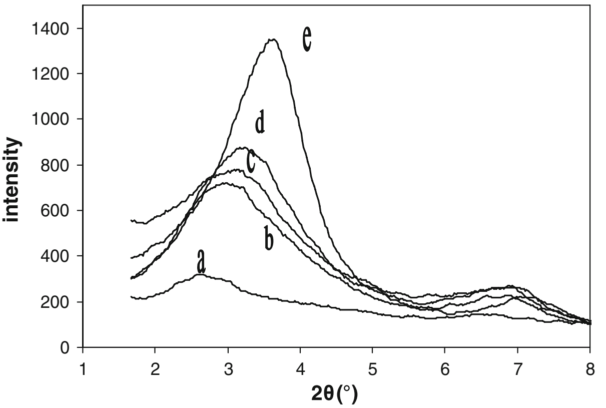

Fig. 2 XRD patterns of **a** sample 6, **b** sample 7, **c** sample 13, **d** sample 8, **e** organoclay

Figure 2 shows XRD patterns of LDPE/POE (75/25) nanocomposites with different OMMT contents and with or without interfacial compatibilization. The LDPE/POE nanocomposite having 1 wt% clay shows a peak around 2.6° corresponding to a basal spacing of 34.6 Å. As compared to the neat clay this sample shows nearly 10Å increase in the d-spacing. This is an indication of a very strong level of intercalation. With increasing of the clay content the increase in d-spacing becomes smaller reaching to 27.6 Å for the nanocomposite samples containing 5 wt% clay. However, even at this high level of clay loading the samples still show characteristics of intercalated structures. Adding PE-g-MA does not change the position of the peak significantly, but results in broadening and intensity decreasing of the peak (comparing c and d). These slight broadening and intensity reduction indicate that the compatibilizer shows its role in better dispersion of clay in the polymeric matrix. However, it seems that this level of compatibilizer is not sufficient for an effective dispersion. Here the ratio of the compatibilizer to the clay is 1:1. But the results indicate that for achieving the full potential of the compatibilizer for an effective exfoliation of clays one should use much higher compatibilizer/clay ratios [25, 26].

The XRD patterns were analyzed and the data are presented in Table 1. As it can be seen the characteristic peak of OMMT in these series of nanocomposites appears almost at the same 2θ, which is probably related to their similar chemical structure.

Morphology characterization using TEM and AFM

Figure 3a–d shows the AFM images of LDPE/POE blends and nanocomposite with different compositions in which different morphological states are seen. These results show that it is possible to distinguish the elastomer particles, i.e. the POE, in the LDPE/POE/OMMT nanocomposites with the AFM technique. A difference in the stiffness of the components at the sample surface can provide images with a phase contrast; this is ideal for polyolefin/elastomer systems in which staining of one component without affecting the other one for TEM characterization is quite difficult due to similarities in molecular structures. As it was mentioned earlier, LDPE and POE have a very similar chemical structure. In these AFM images, soft elastomer particles appear as dark spots while the relatively stiffer LDPE matrix appears bright. As seen from the Fig. 3a, a two-phase morphology is visible for all the systems and POE droplets are dispersed randomly within the LDPE matrix. This is a good example for partially immiscible polymer blend matrix with nonpolar components in which the components have very similar molecular structures. When compatibilizer is added to this system it leads to a distinct reduction in the size of the elastomer particles and to increased irregularities in the particle-shape as shown in Fig. 3b. These apparent changes in the morphology of the elastomer phase may stem from two competing effects during melt-processing; one is rheological in origin while the other stems from a ‘barrier’ effect of the clay particles on rubber particle coalescence [20]. The literature shows that addition of clay to a polymer melt causes an increase in the viscosity [27]. The rheological effect of adding OMMT to LDPE/POE 75/25 nanocomposites will be discussed subsequently. The melt viscosity ratio of the elastomer phase to that of the matrix and the absolute viscosity of the matrix are important factors that control the elastomer particle breakup during melt processing. In principle, an increase in matrix viscosity can alter the balance of droplet breakup versus coalescence in such a way that it produces smaller rubber particles [28]. In addition, Kim et al. have suggested that the presence of clay particles retards the coalescence of small elastomer particles to form larger ones resulting in a net reduction in the elastomer particle size. Their work on the morphology of nylon 6/EPR rubber/clay nanocomposites demonstrated that dispersed clay particles caused a reduction in the size and stability of the dispersed elastomer domains in a nylon 6 matrix via this ‘barrier’ to coalescence mechanism [5]. The amount of discrete rubber particles evidently increases with increasing rubber concentration (see Fig. 3c, d).

The LDPE/POE/OMMT 71.25/23.75/5 nanocomposite was further characterized by TEM and the result is shown in Fig. 4. The dark lines in the TEM images are

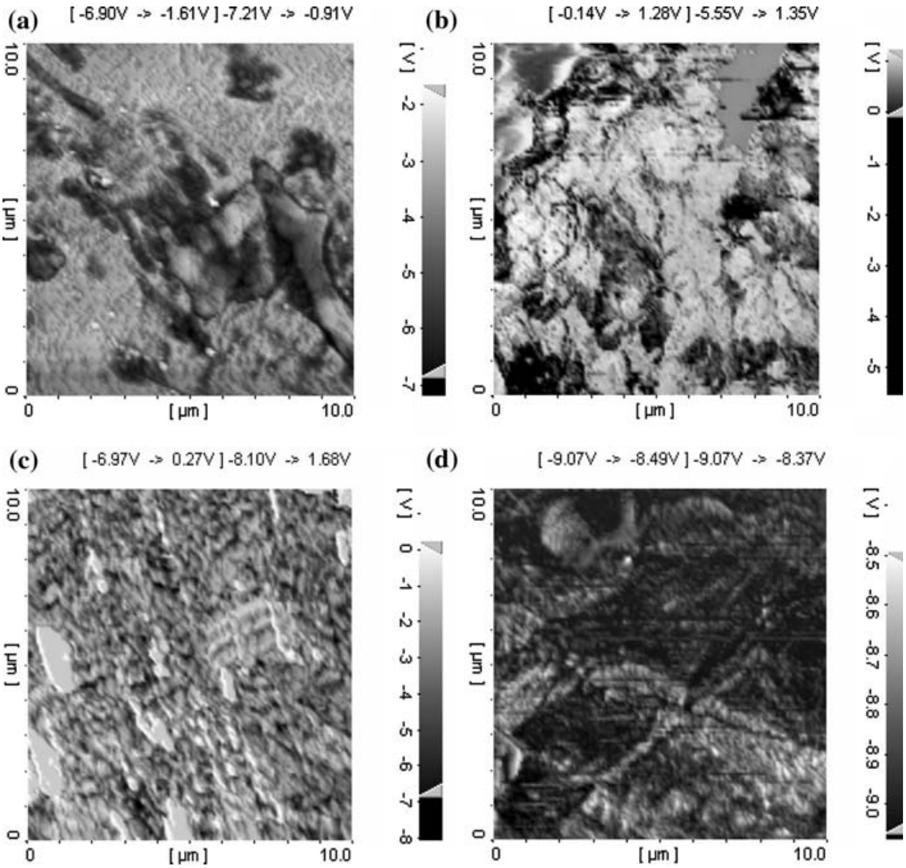

Fig. 3 AFM images of PE/POE blends: **a** 75% LDPE, 25% POE, **b** 71.25% LDPE, 23.75% POE, 5% org-MMT, **c** 50% LDPE, 50% POE and **d** 25% LDPE, 75% POE

clay layers. It is seen that a large portion of the clay layers are in exfoliated state and the remaining portions show intercalated feature. It is also seen that the clay layers exist in both the phases. It seems that the clay layers have partitioned favorably in the POE phase. The large difference in melting points of the POE and LDPE components could be a possible reason for the observed partitioning, because the lower melting point elastomer would tend to wet and to incorporate the clay layers before the LDPE phase melts [29].

Rheological behavior

Rheological behavior of polymer composites in melt state is very critical to understand processability and structure- property relationships of these materials. In rheological tests, first dynamic strain sweep test was applied to nanocomposite samples in order to characterize strain dependence of the viscoelastic properties of the samples and to determine linear viscoelastic region. Since the shear storage

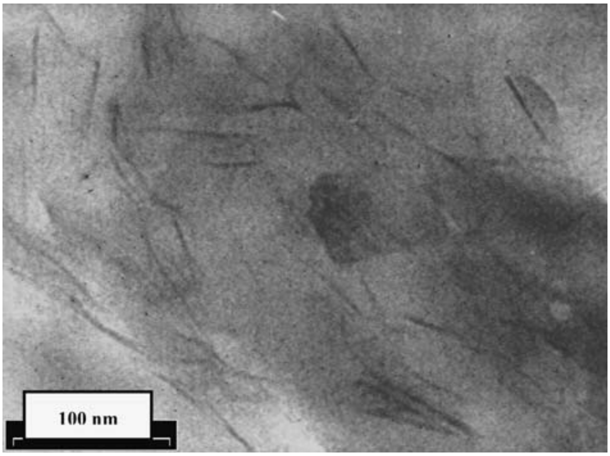

Fig. 4 TEM image of LDPE/POE/OMMT 71.25/23.75/5 nanocomposite

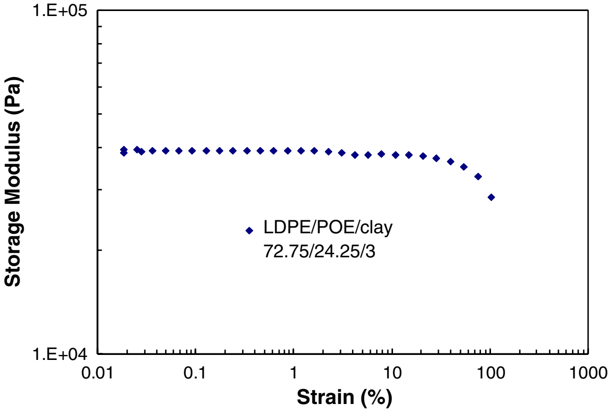

Fig. 5 Storage modulus versus strain (%) curve of the LDPE/POE/clay nanocomposite

modulus (G′) is a more sensitive rheological function than the loss modulus (G″) to the structural changes of the nanocomposites, only the storage modulus curves are presented here. Dependence of storage modulus on the strain for the LDPE/POE 75/25 nanocomposite with 3% OMMT is shown in Fig. 5. Since the cardhouse of nanoplatelets might be destroyed by high shear amplitude, it is necessary to use very low amplitude [30]. The measurements were made with constant shear amplitude of 1%. Dynamic frequency sweep tests were conducted in linear viscoelastic region to further study the microstructural changes of the blends and nanocomposites in detail. The measurement of complex viscosity of blends at low and intermediate frequencies is used to study interactions between phases, because the morphology, in most of the cases, is undisturbed by the flow deformation [31].

Figure 6 depicts the complex viscosity of LDPE, POE and their blends with different compositions. It is seen that the complex viscosity decreases with

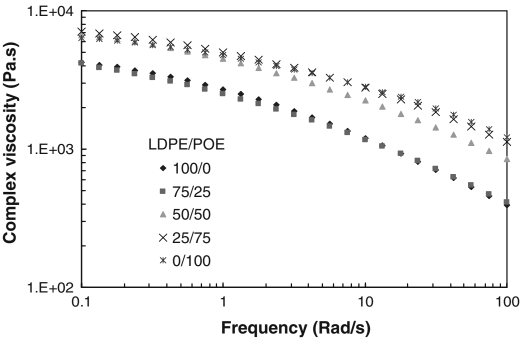

Fig. 6 Complex viscosity versus frequency curves for LDPE/POE blends

increasing of frequency. This is due to the strong shear thinning behavior of the polymers at the molten state. Entanglements between branches and chain segments of POE and LDPE may occur randomly, modifying the entanglement density of these blends under shear flow. Consequently, a nonlinear rheological behavior is observed. It is also seen that POE is more viscose than LDPE and complex viscosity of the blends are intermediate to those of the pure components.

Figure 7 shows the effect of addition of OMMT to LDPE, POE and their blends with various compositions on the complex viscosity and storage modulus of the blends. The complex viscosity and storage modulus of the nanocomposites exhibit an increase at low frequencies as compared to those of the blends. However, the increase in complex viscosity and modulus is not so significant which indicates that this low amount of OMMT has a little effect on restriction of the polymer chain mobility.

Figure 8 demonstrates effect of addition of the different percentage of clay on complex viscosities of LDPE/POE (75/25) nanocomposite systems. From Fig. 8 it can be found that the complex viscosities of the composites increase with increasing of clay loading. Moreover, the effect of adding compatibilizer (PE-g-MA) to the LDPE/POE blend and its nanocomposite is shown in Fig. 8. Addition of compatibilizer in presence of OMMT leads to a drastic increase in complex viscosity. However, when only the compatibilizer alone is added to the LDPE-rich blend system little enhancement in viscosity is seen. This implies that there should be a strong interaction between the clay and the compatibilizer. This could be due to high affinity between the compatibilizer and OMMT which have similar polarities.

The viscosity curves at low frequency region could be fitted by the power law model. The η-ω curves have been used to determine the power law parameters and to explain shear thinning behavior of the polymer nanocomposites at low frequency region [30]. For the frequency sweep data, power law expression is written as

$$\eta = \mathrm{k}\,\omega^{\mathrm{n}} \tag{1}$$

where η is a dynamic viscosity, k is a sample specific pre exponential factor, ω is the oscillation frequency in the frequency sweep test and n is the shear thinning

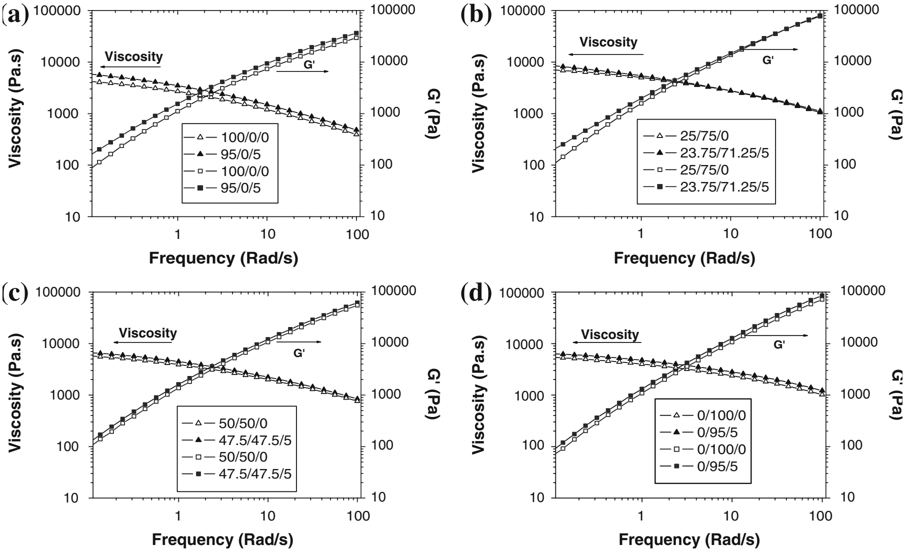

Fig. 7 Comparison of storage modulus (G′) and complex viscosity (η) of blends and nanocomposites with different LDPE/POE/clay composition

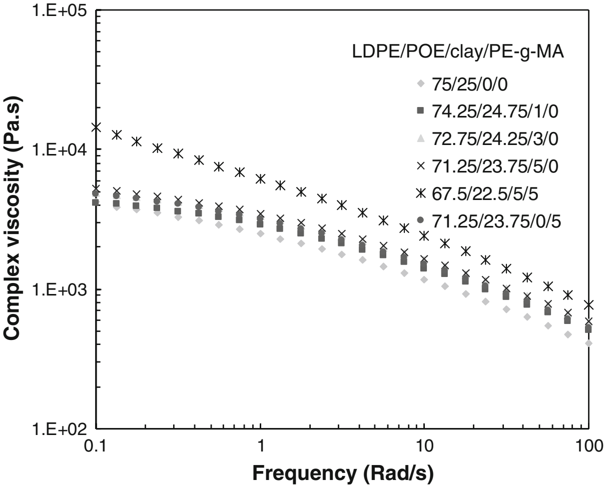

Fig. 8 Effect of compatibilizer and different clay contents on the viscosity of LDPE/POE 75/25 nanocomposites

exponent. k and n can be directly determined from the logarithmic plot of viscosity (η) versus frequency (ω) as follows:

$$\log(\eta) = \log k + n \log(\omega) \tag{2}$$

n is the slope of straight line obtained by plotting log (η) versus log (ω). It is a semi-quantitative measure of the clay dispersion in polymer phase. Wagener and

Reisinger [34] used the value of n as a measure of the degree of exfoliation. In that, it was explicitly assumed that exfoliation leads to a percolated structure which results in a solid-like behavior. Indeed, an increase of the shear thinning exponent is observed with increasing of the degree of exfoliation. In this study, power law model was applied to dynamic viscosity (η) curves of the samples in low-frequency region of 0.1–1 rad/s. The LDPE/POE blend and LDPE/POE/clay nanocomposites did not show significant shear thinning behavior (Fig. 8), resulting in a shear thinning exponent $n = -0.15$. This value indicates a weak exfoliated structure for these nanocomposites. In contrast, the LDPE/POE/clay/PE-g-MA sample does show a pronounced shear thinning. The value of n is −0.38 for this sample which is not an indication for a fully exfoliated structure. These results are in very good agreement with the XRD results. The rheological observation confirms the role of compatibilizer in achieving an improved interaction for this set of nanocomposites.

Figure 9 shows the variation of storage modulus (G′) as a function of frequency for LDPE/POE (75/25) with PE-g-MA and different clay contents. The G′ and loss modulus (G″) of the samples increase with increasing of frequency. This is due to the fact that at low frequency, time is large enough for unraveling of the entanglements therefore a large amount of relaxation occurs which results in low values of storage and loss modulus. However, when a polymer sample is deformed at large frequency the entangled chains do not have time to relax, so modulus goes up.

The changes in G′ by addition of 1, 3, and 5% OMMT to the blend are not significant either. Again adding compatibilizer results in considerable improvement of modulus of the nanocomposite. Low frequency improvement in G′ indicates strong interactions between the clay layers and polymer matrix. The G′ values at $\omega = 0.1$ rad/s are 57, 70, and 77 Pa for LDPE/POE nanocomposites with 1, 3, and 5% OMMT, respectively, but when compatibilizer is added about ten fold increase in the G′ value (i.e. 728 Pa) is seen. These results imply that there is a weak interaction

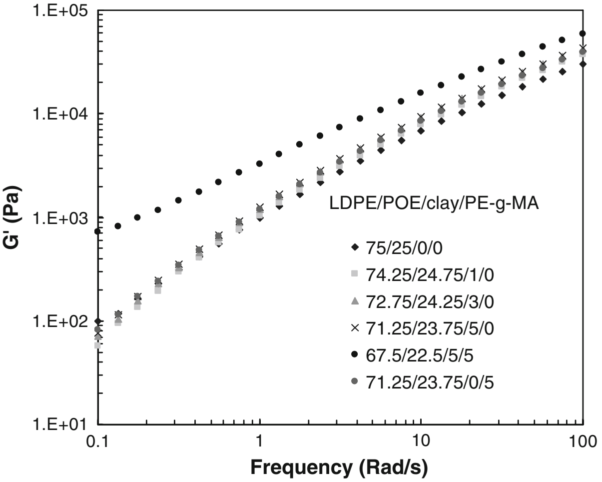

Fig. 9 Effect of compatibilizer and different clay contents on the storage modulus (G′) of LDPE/POE 75/25 nanocomposites

between the OMMT layers and LDPE and POE chains, so that can not show a significant filler effect without a compatibilizer. These results also indicate that clay dispersion and interfacial adhesion are greatly affected by addition of PE-g-MA.

Dynamic mechanical properties

Figure 10 shows plots of loss modulus against temperature for neat polymers, LDPE, POE, and their blends with different compositions. LDPE shows three transitions namely α, β, and γ transitions however, due to the low crystallinity of LDPE, α transition of LDPE is small and broad [32]. POE has only two transitions. Due to the lower crystallinity and the rubbery nature of POE, the α transition, which originates from some type of motion within the crystalline region, is absent for this polymer. Because of the lower crystallinity, and more rubbery like behavior, the β transition for POE (which is related to the motion of methylene groups) takes place at a lower temperature and with a greater intensity as compared to the β transition of LDPE. LDPE/POE blends reveal all the corresponding relaxations. It is seen that by increasing of POE content all the α, β, γ transition peak temperatures shift to a lower temperatures in the blend. Moreover, the β transition peak areas were increased by increasing of POE content confirming the mobility of the amorphous phase.

Table 2 indicates the storage modulus data of all samples at different temperatures. There is a decrease in storage modulus values with increasing of POE content, which is attributed to reduction in crystallinity, as observed by DSC analysis and enhancement of free volume on increase of the POE content.

Figure 11 shows tan δ versus temperature for the LDPE/POE blends. The value of tan δ increases with increase of POE content. In an earlier work [33] a direct correlation between impact properties and tan δ could be established. Using this concept, one can deduce that incorporation of POE improves the impact properties of LDPE.

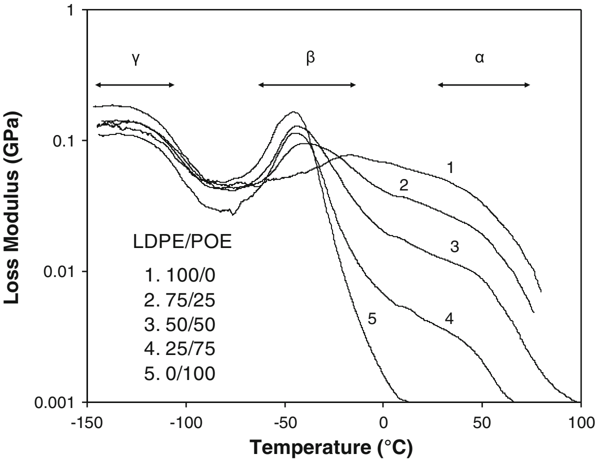

Fig. 10 Loss modulus versus temperature curves for LDPE, POE, and their blends

Table 2 Storage modulus of LDPE, POE, LDPE/POE blends, and LDPE/POE/clay nanocomposites

Sample No.	Storage modulus/GPa				
	−140 °C	−100 °C	−50 °C	0 °C	25 °C
1	3.57	2.40	1.67	0.65	0.34
15	3.35	2.38	1.72	0.65	0.33
5	3.51	2.35	1.55	0.36	0.19
8	3.73	2.49	1.68	0. 39	0.20
14	3.44	2.40	1.61	0.36	0.19
13	4.29	2.90	2.02	0.54	0.28
11	3.37	2.23	1.32	0.17	0.09
12	3.74	2.50	1.48	0.20	0.10
9	2.51	1.66	0.85	0.06	0.03
10	2.99	2.02	1.08	0.08	0.04
2	3.49	2.12	0.84	0.03	0.02
16	4.08	2.78	1.18	0.04	0.02

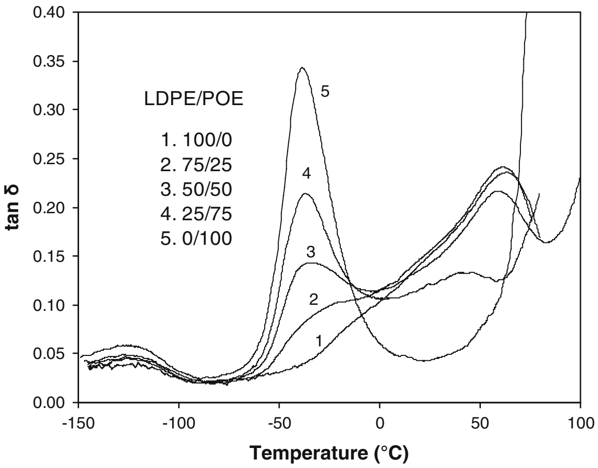

Fig. 11 tan δ versus temperature curves for LDPE/POE blends

The storage modulus of the LDPE/POE blends and nanocomposites at different temperature regions are shown in Table 2. As it can be seen the storage modulus of the nanocomposites are higher than their neat blends indicating the reinforcing role of clay. OMMT anchors at different positions in the matrix, thus restricting the movement of the chains. This enhancement of modulus is more noticeable in POE nanocomposites, which is in agreement with the XRD results. It was demonstrated that POE nanocomposites had more exfoliated clay structure as compared to LDPE nanocomposites. As it is seen from Table 2, at temperatures higher than glass transition temperature (T_g) of POE (−50 °C) storage modulus of the POE/OMMT (95/5) nanocomposite is about 50% higher than that of the neat POE. The enhancement of storage modulus strongly depends on the aspect ratio of the dispersed clay layers and the intercalation of the polymer chains inside the clay matrix. When polymer matrix is reinforced with a rigid filler the polymer interface adjacent to the clay particle is highly restrained mechanically. Active surface area of the filler increases due to the intercalation of the polymer chains inside the clay galleries. Polymer chains inside the clay galleries are immobilized and the effective immobilization of these chains is responsible for the enhancement of the hydrodynamic storage modulus [34].

Table 2 also demonstrates the effect of interfacial compatibilization on storage modulus by incorporating 5 wt% PE-g-MA into the LDPE/POE/clay nanocomposite. It is observed that the storage modulus of LDPE/POE/clay/PE-g-MA is higher than that of LDPE/POE/clay. The increment of storage modulus is related to the better dispersion of clay. In line with the XRD results, DMTA results also indicate that the addition of PE-g-MA as a compatibilizer enhances the intercalation of polymer chains into the clay gallery by the presence of a polar maleic group in PE-g-MA.

Conclusion

LDPE/POE/OMMT nanocomposites could be prepared via a simple direct melt compounding. PE-g-MA acted as an effective compatibilizer for clay dispersion. XRD patterns confirmed presence of different levels of intercalated structures for all the nanocomposites. TEM results revealed existence of clay layers in both phases but they were mainly localized in the POE phase. AFM micrographs confirmed presence of phase separated morphology and showed that phase inversion occurs when the percentage of POE in the blends is more than 60%. Adding OMMT to the blends led to a reduction in the size of POE phase. Rheological results revealed that POE was more viscose than LDPE and all samples showed shear thinning behavior. Clear correlation between the shear thinning behavior and extent of exfoliation was observed. The rheological behavior of the nanocomposites changed from a liquid-like to a solid-like when the structure changed from a phase separated state to an intercalated and/or an exfoliated structure possibly due to percolation. Changes in the complex viscosity and storage modulus were not significant in the LDPE/POE/clay nanocomposites without compatibilizer. In contrast, the LDPE/POE 75/25 nanocomposites with 5 wt% OMMT in presence of compatibilizer exhibited significantly high storage and loss modulus as well as complex viscosity at the whole frequency range studied. DMTA results indicated that the storage modulus of the nanocomposites were higher than their pristine blends. This was attributed to the good interaction between the clay layers and the matrix. The enhancement of storage modulus was more noticeable in POE and LDPE/POE/clay/PE-g-MA nanocomposites which were in good agreement with the XRD results. This showed that POE and LDPE/POE/clay/PE-g-MA nanocomposites had more exfoliated structure as compared to LDPE and LDPE/POE/clay nanocomposites, respectively. Our results demonstrate that adding clay to polymer blends allows tailoring the final properties of the hybrid, potentially leading to high-performance materials which combine the advantages of polymer blends and the merits of polymer nanocomposites.

Acknowledgments Financial support from Iranian Nanotechnology Initiative is highly appreciated.

References

1. Moussaif N, Groeninckx G (2003) Nanocomposites based on layered silicate and miscible PVDF/PMMA blends: melt preparation, nanophase morphology and rheological behaviour. Polymer 44:7899
2. Filippone G, Dintcheva NT, Acierno D, La Mantia FP (2008) The role of organoclay in promoting co-continuous morphology in high-density poly(ethylene)/poly(amide) 6 blends. Polymer 49:1312
3. Feng M, Gong FL, Zhao C, Chen G, Zhang S, Yang M (2004) Effect of clay on the morphology of blends of poly(propylene) and polyamide 6/clay nanocomposites. Polym Int 53:1529
4. Li YJ, Shimizu H (2005) Co-continuous polyamide 6 (PA6)/acrylonitrile-butadiene-styrene (ABS) nanocomposites. Macromol Rapid Commun 26:710
5. Khatua BB, Lee DJ, Kim HY, Kim JK (2004) Effect of organoclay platelets on morphology of nylon-6 and poly(ethylene-ran-propylene) rubber blends. Macromolecules 37:2454
6. Hotta S, Paul DR (2004) Nanocomposites formed from linear low density polyethylene and organoclays. Polymer 45:7639
7. Liu Y, Kontopoulou M (2006) The structure and physical properties of polypropylene and thermoplastic olefin nanocomposites containing nanosilica. Polymer 47:7731
8. Defeng W, Lanfeng W, Ming Z, Weidong Z, Yisheng Z (2008) Morphology evolution of nanocomposites based on poly(phenylene sulfide)/poly(butylene terephthalate) blend. J Polym Sci Polym Phys 46:1265
9. As'habi L, Jafari SH, Baghaei B, Khonakdar HA, Pötschke P, Böhme F (2008) Structural analysis of multicomponent nanoclay-containing polymer blends through simple model systems. Polymer 49:2119
10. Zou H, Zhang Q, Tan H, Wang K, Du R, Fu Q (2006) Clay locked phase morphology in the PPS/PA66/clay blends during compounding in an internal mixer. Polymer 47:6
11. Lee MH, Dan CH, Kim JH, Cha J, Kim S, Hwang Y, Lee CH (2006) Effect of clay on the morphology and properties of PMMA/poly(styrene-co-acrylonitrile)/clay nanocomposites prepared by melt mixing. Polymer 47:4359
12. Acharya H, Srivastava SK, Bhowmick AK (2006) Ethylene propylene diene terpolymer/ethylene vinyl acetate/layered silicate ternary nanocomposite by solution method. Polym Eng Sci 46:837
13. Rajkiran TR, Kartic KC, Upendra N (2008) New poly(phenylene oxide)/polystyrene blend nanocomposites with clay: intercalation, thermal and mechanical properties. J Appl Polym Sci 108:1818
14. Lim JW, Hassan A, Rahmat AR, Wahit MU (2006) Rubber-toughened polypropylene nanocomposite: effect of polyethylene octene copolymer on mechanical properties and phase morphology. J Appl Polym Sci 99:3441
15. López-Quintanilla ML, Sánchez-Valdés S, Ramos de Valle LF, Guedea Miranda R (2006) Preparation and mechanical properties of PP/PP-g-MA/Org-MMT nanocomposites with different MA content. Polym Bull 57:385
16. Kato M, Okamoto H, Hasegawa N, Tsukigase A, Usuki A (2003) Preparation and properties of polyethylene-clay hybrids. Polym Eng Sci 43:1312
17. Dow Plastics (2001) Trademark of The Dow Chemical Company Published
18. Mishra JK, Hwang KJ, Ha CS (2005) Preparation, mechanical and rheological properties of a thermoplastic polyolefin (TPO)/organoclay nanocomposite with reference to the effect of maleic anhydride modified polypropylene as a compatibilizer. Polymer 46:1995
19. Mehta S, Mirabella FM, Rufener K, Bafna A (2004) Thermoplastic olefin/clay nanocomposites: morphology and mechanical properties. J Appl Polym Sci 92:928
20. Lee H, Fasulo PD, Rodgers WR, Paul DR (2005) TPO based nanocomposites. Part 1. Morphology and mechanical properties. Polymer 46:11673
21. Maiti M, Bandyopadhyay A, Bhowmick AK (2006) Preparation and characterization of nanocomposites based on thermoplastic elastomers from rubber-plastic blends. J Appl Polym Sci 99:1645
22. Morawiec J, Pawlak A, Slouf M, Galeski A, Piorkowska E, Krasnikowa N (2005) Preparation and properties of compatibilized LDPE/organo-modified montmorillonite nanocomposites. Euro Polym J 41:1115

23. Tanniru M, Yuan Q, Misra RDK (2006) On significant retention of impact strength in clay–reinforced high-density polyethylene (HDPE) nanocomposites. Polymer 47:2133
24. Lew CY, Murphy WR, McNally M (2004) Preparation and properties of polyolefin-clay nanocomposites. Polym Eng Sci 44:1027
25. Chrissopoulou K, Altintzi I, Anastasiadis SH, Giannelis EP, Pitsikalis M, Hadjichristidis N, Theophilou N (2005) Controlling the miscibility of polyethylene/layered silicate nanocomposites by altering the polymer/surface interactions. Polymer 46:12440
26. Joshi M, Viswanathan V (2006) High-performance filaments from compatibilized polypropylene/clay nanocomposites. J Appl Polym Sci 102:2164
27. Galgali G, Ramesh C, Lele A (2001) A rheological study on the kinetics of hybrid formation in polypropylene nanocomposites. Macromolecules 34:852
28. Wu S (1987) Chain entanglement and melt viscosity of compatible polymer blends: poly(methyl methacrylate) and poly(styrene-acrylonitrile). Polymer 28:1144
29. Austin JR, Kontopoulou M (2006) Effect of organoclay content on the rheology, morphology, and physical properties of polyolefin elastomers and their blends with polypropylene. Polym Eng Sci 46:1491
30. Wagener R, Reisinger TJG (2003) A rheological method to compare the degree of exfoliation of nanocomposites. Polymer 44:7513
31. Guimaraes OC, Coutinho MB, Rocha CG, Farah M, Bretas ES (2002) Rheological and morphological properties of high-density polyethylene and poly(ethylene-octene) blends. J Appl Polym Sci 86:2240
32. Khonakdar HA, Wagenknecht U, Jafari SH, Hässler R, Eslami H (2004) Dynamic mechanical properties and morphology of polyethylene/ethylene vinyl acetate copolymer blends. Adv Polym Tech 23:307
33. Jafari SH, Gupta AK (2000) Impact strength and dynamic mechanical properties correlation in elastomer-modified polypropylene. J Appl Polym Sci 78:962
34. Vu YT, Mark JE, Pham LH, Engelhart MJ (2001) Clay nanolayer reinforcement of cis-1,4-polyisoprene and epoxidized natural rubber. J Appl Polym Sci 82:1391